Available online at www.sciencedirect.com
ScienceDirect
Journal of Sound and Vibration 322 (2009) 785–797
JOURNAL OF SOUND AND VIBRATION
www.elsevier.com/locate/jsvi

The effect of long-wavelength stiffness variation on wear pattern generation

N.P. Hoffmann[a,*], M. Ciavarella[b,1], U. Stolz[c,2], C. Weiß[a]

[a]*Mechanics and Ocean Engineering, Hamburg University of Technology, Eißendorfer Straße 42, 21073 Hamburg, Germany*
[b]*Politecnico di Bari, Viale Gentile 182, 70125 Bari, Italy*
[c]*Robert Bosch GmbH, Corporate Research, CR/ARU2, P.O. Box 10 60 50, 70049 Stuttgart, Germany*

Received 7 January 2008; received in revised form 17 November 2008; accepted 17 November 2008
Handling Editor: M.P. Cartmell
Available online 1 January 2009

Abstract

In many systems with moving contacts spatially periodic wear patterns related to structural resonances emerge. Often, however, the structural properties of the sliding system vary periodically with position. Based on a generic minimal model the present work investigates the effect of a spatially periodic structural stiffness on wear pattern generation. Linear stability of the resulting wear dynamics is analysed using spatial Floquet analysis. It turns out that the emergence of wear patterns by instability can in general not be evaluated through stability analysis based on spatially local parameters alone. A spatially periodic stiffness can stabilize the system, depending on the wavelength and the amplitude of the spatially periodic parameter variation. The relevance of the effect is discussed and open points are addressed.

1. Introduction

Wear patterns are found in a large number of application fields: dust roads evolve into "washboard"-patterns [1], brake rotors develop uneven surfaces [2], hard disk drives are affected. The most classical field of wear pattern generation, however, is found in train–track interaction. In that field various potential explanations have been proposed and many aspects of the complex problem have been studied (Sato et al. [3] estimate about 1500 papers), involving mainly the dynamics of the train and the response of the track, with the contact mechanics generally playing the role of nonlinear stiffness and contact "filter" of too short wavelengths, but also involving metallurgical aspects, different wear laws, etc. Yet, the phenomenon is not fully understood, perhaps because some fundamental phenomena and mechanisms are still to be captured [4]: specifically, it is still not clear if the wavelength selection occurs due to a given structural frequency, driven by a vertical or torsional resonance of the system, due to a multi-degree-of-freedom effect, where a single

*Corresponding author. Tel.: +49 40 42878 3120; fax: +49 40 42878 2028.
E-mail addresses: norbert.hoffmann@tuhh.de, norbert.hoffmann@tu-harburg.de (N.P. Hoffmann), mciava@poliba.it (M. Ciavarella), ulrich.stolz@de.bosch.com (U. Stolz).
[1]Tel.: +39 80 596 2811; fax: +39 80 596 2777.
[2]Tel.: +49 711 811 6915; fax: +49 711 811 267 650.

0022-460X/$ - see front matter © 2008 Elsevier Ltd. All rights reserved.
doi:10.1016/j.jsv.2008.11.027

frequency is filtered out by some criteria, or if the wavelength of the corrugation pattern is just not due to a given structural frequency at all (see especially Refs. [4,5]).

Of the many potential causes of corrugation, the discrete spacing of the supports has sometimes attracted attention. For example Frederick and Bugden [6] reported that a test section on a British Rail main line with continuously supported track has not shown any signs of corrugation, whereas the neighbouring track supported on sleepers was heavily corrugated. Corrugation may, however, also arise in systems with continuous support.

A recent investigation in the London Underground Victoria Line [7] is another interesting case to mention. The results show the possibility of a superposition of long- and short-wave corrugation at the same location. The long corrugation is of about 300–400 mm wavelength which corresponds to frequencies in the range 50–100 Hz, which is typical of the resonance of the vehicle's unsprung mass on the track stiffness (which is commonly called "P2 resonance"); the second wavelength is about 30–40 mm whose frequency corresponds (the authors say "exactly") to the "pinned–pinned resonance", in which the rail vibrates almost as if it were a beam pinned at sleepers. In curves with higher traction, however, the long wavelength disappears, and another peak of corrugation appears in the range 60–80 mm, which the authors do not discuss, which would, however, correspond to corrugation at about 250–500 Hz. To summarize, the data presented by Grassie et al. [7] seems to suggest that in addition to the aspects related to P2 or pinned–pinned resonance alone, additional aspects have to be looked for. Along the same reasoning, for example Diana et al. [8] report an investigation for a similar metro system (in Milano), which does not show evidence of either resonance being directly responsible for corrugation. Instead they develop a model with a vertical and a torsional degree of freedom including a track with spatially varying stiffness to take into account the presence of sleepers. Time domain simulations do result in corrugation patterns, depending on the choice of parameters. Therefore Diana et al. [8] proposed a "triggering" mechanism based on the discrete nature of the support and its periodic change of stiffness.

As mentioned already, next to rail corrugation, there are also other lines of research on the topic of wear pattern generation; e.g. there is the case of "washboarding" of dust roads [1,9], or the generation of wear patterns in friction brakes [2]. The present work has originally been motivated by the latter problem. Since also in braking systems underlying stiffness variations, e.g. due to mounting conditions or properties of brake disks, do appear, this paper readdresses the problem of wear pattern generation in the presence of spatially varying stiffness properties. Instead of using a time-domain approach (as. e.g. also Ref. [8]), the use of Floquet analysis [10] is attempted. The model to be used will be highly abstracted to allow evaluation of the analysis technique. The primary objectives of the present study therefore are to (1) gain insight into the nature of wear pattern generation in systems with long-wavelength stiffness variations and to (2) evaluate feasibility of the Floquet type approach presented.

The paper is structured as follows: First a single-degree-of-freedom model is introduced that has already been used previously to study fundamental dynamical properties of wear pattern generation. The model is extended to allow for spatially periodic stiffness characteristics. The linear stability of the system is then analysed using Floquet analysis and results are presented. Finally, the findings are discussed and aspects not considered yet are addressed.

2. The model and the computational approach

A single-degree-of-freedom linear harmonic oscillator sliding with a constant horizontal speed V over an originally plane surface is considered as generic model. The surface is subjected to wear due to the power generated by the action of the friction force due to repeated interaction of the sliders with the surface. Due to the coupling of structural properties with the wear evolution wear patterns may emerge, see Fig. 1. The model has already been used frequently to analyse fundamental properties of wear pattern generation (compare e.g. Refs. [1,2,11]) and we refer to the original studies for additional aspects on wear pattern generation in general. For the purpose of the present investigation the stiffness parameter $K = K(x)$ is assumed to vary periodically in space to model underlying parameter variations, e.g. due to compliance variations of the counter-surface. Of course the model is highly abstracted from any real world application. The purpose of the present study does, however, not lie in quantitative prediction, but rather in analysing fundamental effects of spatial

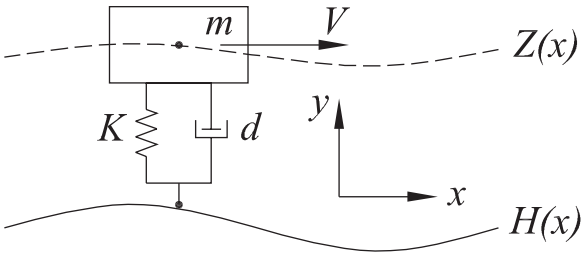

Fig. 1. Single-degree-of-freedom model.

parameter variations on wear pattern generation. The abstraction thus serves to focus on the stability aspects rather than on the specifics of an application system at hand.

The mass m of the oscillator is coupled to the surface through a linear viscous damping element with damping constant d and a linear spring with spring stiffness K. In the following a spatial variation $K = K(x)$ of this stiffness is assumed. $Z(x)$ denotes the vertical position of the mass and $H(x)$ the height of the counter-surface at the momentary position x of the mass. The evolution equation for the structural oscillation of the mass at its position reads

$$m\frac{\mathrm{D}^2}{\mathrm{D}t^2}Z + d\frac{\mathrm{D}}{\mathrm{D}t}(Z-H) + K(x)(Z-H) = 0, \tag{1}$$

where $\mathrm{D}/\mathrm{D}t$ stands for the derivative evaluated at the momentary position of the mass—i.e. the "material derivative". For the analysis the equation is divided by m and a natural undamped (angular) frequency $\omega_0 = \sqrt{K/m}$ is introduced. To connect the discrete oscillator model with the spatio-temporal wear dynamics, the model of the moving oscillator is replaced by an ensemble of moving oscillators, such that the ordinary differential equation (1) can be replaced by a partial differential equation to be coupled with a wear evolution equation for the wear surface to be specified later. For this the material derivative $\mathrm{D}/\mathrm{D}t$ is evaluated as $\mathrm{D}/\mathrm{D}t = \partial_t + V\partial_x$, where V stands for the (advection) velocity of the oscillator relative to the surface. The resulting equation in the Eulerian frame reads

$$(\partial_t + V\partial_x)^2 Z(x,t) + (d/m)(\partial_t + V\partial_x)(Z(x,t) - H(x,t)) + \omega_0^2(x)(Z(x,t) - H(x,t)) = 0. \tag{2}$$

Wear is assumed to follow an Archard type wear model, which in the present formulation may be expressed through assuming proportionality for the rate of change in surface height (i.e. wear) to the power generated due to friction for a given surface area. The friction force of the present model is assumed to be proportional to the normal load and the relative sliding velocity V is assumed to be constant. The resulting local wear is thus proportional to the local normal load the oscillator exerts on the sliding surface. Of course this assumption on wear is highly restrictive. However, as for the high level of abstraction of the structural system, also with respect to the wear model a strong abstraction seems appropriate. The purpose of the present work lies in showing a general approach and general results for the case of spatially varying parameters in the context of wear pattern generation. The approach might then later be extended also to more realistic, but possibly also more problem specific, structural and wear models, like e.g. the $T\gamma$ model [12,13].

With the normal load as $m[g + (\partial_t + V\partial_x)^2 Z]$ the surface evolution equation is

$$\partial_t H(x,t) = -ma(H)[g + (\partial_t + V\partial_x)^2 Z(x,t)], \tag{3}$$

where a factor $a(H)$ parameterizes the wear rate as a function of the surface height to allow for a dependency of the wear rate on the state of the surface topography.

Eqs. (2) and (3) form a set of equations describing both the dynamics of the oscillator as well as the wear evolution of the counter-surface. As usual in such spatio-temporal problems (basically to allow application of Floquet analysis) the fields are now decomposed into a component corresponding to a spatial mean value, depending on time only, and into the deviation from that mean, i.e.

$$H(x,t) = H_0(t) + h(x,t), \quad Z(x,t) = Z_0(t) + z(x,t), \tag{4}$$

with $h(x,t)$ and $z(x,t)$ having a vanishing spatial average, $\overline{h(x,t)}=0$, $\overline{z(x,t)}=0$, where the overline denotes a spatial average. To investigate the stability of a spatially homogeneous wear evolution around the spatially averaged surface height $H_0(t)$, the nonlinear wear equation is linearized with respect to the spatially dependent variables. Then equations for $H_0(t)$, $Z_0(t)$, $h(x,t)$ and $z(x,t)$ are derived in the usual way. The result is

$$\partial_t H_0 = -ma(H_0)[g+\partial_{tt}^2 Z_0], \tag{5a}$$

$$\partial_t h = -m\left.\frac{\partial a}{\partial H}\right|_{H_0} h(g+\partial_{tt}Z_0) - ma(H_0)(\partial_t + V\partial_x)^2 z, \tag{5b}$$

$$\partial_{tt}^2 Z_0 + (d/m)\partial_t(Z_0-H_0) + \overline{\omega_0^2}(Z_0-H_0) + \overline{\omega_0^2(z-h)} = 0, \tag{6a}$$

$$(\partial_t + V\partial_x)^2 z + (d/m)(\partial_t + V\partial_x)(z-h) + \omega_0^2(x)(z-h) + [\omega_0^2 - \overline{\omega_0^2}](Z_0-H_0) - \overline{\omega_0^2(z-h)} = 0. \tag{6b}$$

To simplify notation, later on sometimes the parameter $\beta = mg\partial a/\partial H|_{H_0}$ will be used in Eq. (5b). Here it stands for a possible dependency of the wear rate on the amount of wear that has already happened at a certain position and thus brings into play a nonlinearity.

At first sight the resulting system seems to be strongly coupled. However, as has largely been shown previously (e.g. Ref. [1]), using some plausible assumptions the equations can be decoupled. For that purpose we first neglect the term $\partial_{tt}Z_0$ due to its smallness and the implicit time-dependency of $a(H_0(t))$ due to the slowness of the wear process. Then one can note that the non-local term $\overline{\omega_0^2(z-h)}$ can have a non-vanishing contribution only if the resulting $(z-h)$ has a spectral component also contained in ω_0^2. Since the present paper focuses on variations of stiffness that are much longer than the wavelength of the appearing corrugation, the term is neglected in the following. Additional justification of this assumption will later on be gained from the results obtained. The last assumption consists in neglecting the term $[\omega_0^2 - \overline{\omega_0^2}](Z_0-H_0)$ in Eq. (6b): following the previous assumptions, it can be seen from Eq. (6a) that (Z_0-H_0) approaches zero, thus allowing omission of the corresponding term also in Eq. (6b).

Finally, Eqs. (5b) and (6b) for the spatially inhomogeneous variables h and z decouple completely from Eqs. (5a) and (6a). In addition, (5b) and (6b) form a linear system of equations periodic in space, such that they summarize a stability problem for wear pattern generation that can be approached by spatial Floquet analysis.

When ω_0^2 is spatially homogeneous, a straightforward eigenvalue problem results that has been analysed previously (cf. Refs. [1,2]). In the following we assume ω_0^2 to vary periodically with some wavelength L, i.e. $\omega_0^2(x) = \omega_0^2(x+L)$. Solutions of the linear differential equations with spatially periodic coefficients can then be expressed in terms of a Floquet decomposition,

$$h(x,t) = \hat{h}(x)\exp(\mathrm{i}kx)\exp(st), \quad z(x,t) = \hat{z}(x)\exp(\mathrm{i}kx)\exp(st), \tag{7}$$

where the functions are decomposed into the product of a function with the same periodicity as the underlying equations, i.e. $\hat{h}(x) = \hat{h}(x+L)$ and $\hat{z}(x) = \hat{z}(x+L)$, and a harmonic component $\exp(\mathrm{i}kx)$ with a so-called Floquet wavenumber k [10].

To numerically treat the resulting system, a Galerkin technique may be employed. For that purpose $\hat{h}$ and $\hat{z}$ are expanded as Fourier series,

$$\hat{h}(x) = \sum_{n=0}^{\infty} h_n \exp(\mathrm{i}n\alpha x), \quad \hat{z}(x) = \sum_{n=0}^{\infty} z_n \exp(\mathrm{i}n\alpha x), \tag{8}$$

where $\alpha = 2\pi/L$ is the prescribed wavenumber of the underlying parameter variation.

In principle, an infinite number of Fourier modes is necessary. In the numerical representation the Fourier sum is, however, truncated at a certain number N of modes. In the course of the numerical analysis it has then to be assured that sufficient convergence has been reached, such that resulting eigenvalues and eigenvectors

remain substantially unaffected by a further increase of the truncation parameter N. For the results presented below N has been chosen appropriately, up to values of $N = 24$.

After substituting the functions of Eqs. (7) and (8) into Eqs. (5b) and (6b) we obtain algebraic equations for the coefficients h_n, z_n by Galerkin projections: (i) the equations are multiplied by $\exp(-\mathrm{i}\tilde{n}\alpha x)$ and (ii) integrated over the spatial periodicity interval: $(1/L)\int \ldots \mathrm{d}x$.

Following this procedure, inserting the Floquet decompositions into the equations for h, i.e. Eq. (5b), yields

$$\begin{aligned} 0 = {} & sh + \beta h + ma(H_0)\left[s^2 z + 2sV(\mathrm{i}k)z + 2sV\left(\sum_n z_n(\mathrm{i}n\alpha)\exp(\mathrm{i}n\alpha x)\right)\exp(\mathrm{i}kx)\exp(st)\right] \\ & + V^2(\mathrm{i}k)^2 z + 2V^2(\mathrm{i}k)\sum_n z_n(\mathrm{i}n\alpha)\exp(\mathrm{i}n\alpha x)\exp(\mathrm{i}kx)\exp(st) \\ & + V^2\sum_n z_n(\mathrm{i}n\alpha)^2\exp(\mathrm{i}n\alpha x)\exp(\mathrm{i}kx)\exp(st). \end{aligned} \tag{9}$$

After Galerkin projection, dropping the common terms $\exp(st)$ and sorting the result slightly, the following algebraic equations result:

$$sh_{\tilde{n}} = -\beta h_{\tilde{n}} - ma(H_0)\{s^2 + 2sV(\mathrm{i}k) + 2sV(\mathrm{i}\tilde{n}\alpha) + V^2(\mathrm{i}k)^2 + 2V^2(\mathrm{i}k)(\mathrm{i}\tilde{n}\alpha) + V^2(\mathrm{i}\tilde{n}\alpha)^2 z_{\tilde{n}}\}. \tag{10}$$

Analogously Eq. (6b), i.e. the z-equation can be evaluated. After introducing the corresponding Floquet products, the result is

$$\begin{aligned} 0 = {} & s^2 z + 2sV(\mathrm{i}k)z + 2sV\left(\sum_n z_n(\mathrm{i}n\alpha)\exp(\mathrm{i}n\alpha x)\right)\exp(\mathrm{i}kx)\exp(st) \\ & + V^2(\mathrm{i}k)^2 z + 2V^2(\mathrm{i}k)\sum_n z_n(\mathrm{i}n\alpha)\exp(\mathrm{i}n\alpha x)\exp(\mathrm{i}kx)\exp(st) \\ & + V^2\sum_n z_n(\mathrm{i}n\alpha)^2\exp(\mathrm{i}n\alpha x)\exp(\mathrm{i}kx)\exp(st) \\ & + \frac{d}{m}\left[s(z-h) + V(\mathrm{i}k)(z-h) + V\sum_n (z_n - h_n)\exp(\mathrm{i}n\alpha x)\exp(\mathrm{i}kx)\exp(st)\right] \\ & + \omega_0^2(x)(z-h). \end{aligned} \tag{11}$$

After Galerkin projection and dropping $\exp(st)$:

$$\begin{aligned} 0 = {} & [s^2 + 2sV(\mathrm{i}k) + 2sV(\mathrm{i}\tilde{n}\alpha) + V^2(\mathrm{i}k)^2 + 2V^2(\mathrm{i}k)(\mathrm{i}\tilde{n}\alpha)z_{\tilde{n}} + V^2(\mathrm{i}\tilde{n}\alpha)^2]z_{\tilde{n}} + \frac{d}{m}[s + V(\mathrm{i}k) + V(\mathrm{i}\tilde{n}\alpha)](z_{\tilde{n}} - h_{\tilde{n}}) \\ & + \frac{1}{L}\int_0^L \omega_0^2(x)\sum_n (z_n - h_n)\exp(\mathrm{i}(n-\hat{n})\alpha x)\,\mathrm{d}x. \end{aligned} \tag{12}$$

Since Eq. (6b) for z contained the spatially dependent function $\omega_0^2(x)$ there do remain integrals over x to be evaluated. A simple way to proceed is to decompose the spatially dependent function $\omega_0^2(x)$ into a Fourier series,

$$\omega_0^2(x) = \sum_{m=-\infty}^{\infty} \hat{\omega}_m \exp(\mathrm{i}m\alpha x), \quad \hat{\omega}_{-m} = \hat{\omega}_m^*, \tag{13}$$

where the given relations for the expansion coefficients have to be taken into account to ensure a real-valued function.

Using $(1/L)\int_0^L \exp(\mathrm{i}(m+n-\hat{n})\alpha x)\,\mathrm{d}x = \delta_{m(\hat{n}-n)}$, the remaining integrals of the Galerkin projection can then be evaluated in terms of convolution sums:

$$\begin{aligned}\frac{1}{L}\int_0^L \sum_{m=-\infty}^{\infty} \hat{\omega}_m \exp(\mathrm{i}m\alpha x) \sum_{n=0}^{\infty}(z_n - h_n)\exp(\mathrm{i}(n-\hat{n})\alpha x)\,\mathrm{d}x \\ = \sum_{m=-\infty}^{\infty}\sum_{n=0}^{\infty}\frac{1}{L}\int_0^L \hat{\omega}_m(z_n - h_n)\exp(\mathrm{i}(m+n-\hat{n})\alpha x) \\ = \sum_{n=0}^{\infty}\hat{\omega}_{\hat{n}-n}(z_n - h_n). \end{aligned} \tag{14}$$

In principle, any periodic function $\omega_0^2(x)$ that may be represented by a Fourier expansion could be used. For the present investigation a harmonically varying stiffness is assumed: $\omega_0^2(x) = \hat{\omega}_0 + \hat{\omega}_1\exp(\mathrm{i}\alpha x) + \hat{\omega}_1^*\exp(-\mathrm{i}\alpha x)$. The convolution sums then collapse and the resulting algebraic system of equations can be set up in a straightforward manner. After collecting all equations and assembling them a quadratic eigenvalue problem of the form

$$Ax + sBx + s^2Cx = 0 \tag{15}$$

results, where $x = [h_1\ h_2\ \ldots\ h_N\ z_1\ z_2\ \ldots\ z_N]^{\mathrm{T}}$, N is the truncation parameter of the underlying Fourier expansions and A, B and C are corresponding coefficient matrices.

As has already been pointed out, when the eigenvalue problem is solved, it has to be ensured that N is chosen large enough to obtain sufficiently converged eigenvalues and eigenvectors.

3. Results

To introduce the results of an underlying stiffness variation, Fig. 2 first summarizes the stability behaviour for vanishing stiffness variation. In the present framework the spectral results, presented already earlier (see e.g. Ref. [2]), can be obtained by setting the truncation parameter in the Floquet expansion to $N = 0$. It then turns out that the system has three fundamental modes. Two of them are just the vibration modes of the moving oscillator, one of them can be identified as the surface evolution mode. The vibration modes are damped according to the prescribed damping parameter and yield frequencies depending on the Floquet wavenumber according to the change from the Lagrangian to the Eulerian coordinate frame: to understand

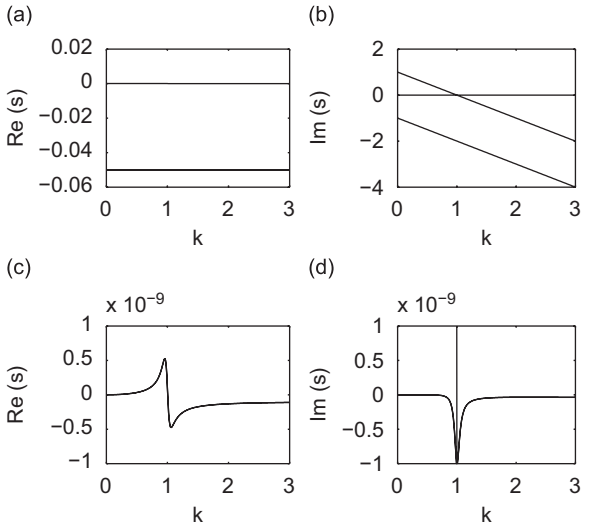

Fig. 2. Results for vanishing inhomogeneity for $m = 1\,\mathrm{kg}$, $\hat{\omega}_0 = 1\,\mathrm{s}^{-2}$, $a_0 = a(H_0) = 10^{-10}\,\mathrm{s\,kg}^{-1}$, $V = 1\,\mathrm{m\,s}^{-1}$, $\beta = 0.0\,\mathrm{s}^{-1}$ and $d/m = 0.1\,\mathrm{kg\,ms}^{-1}$. (a) and (b) show the full range, (c) and (d) give magnified views of the eigenvalues corresponding to surface evolution.

why the resulting frequencies in Fig. 2b decrease linearly with k, one could note that a stationary displacement pattern has to result when a harmonic $z(x)$ is chosen with a wavelength corresponding just to the distance the slider travels during its period; for $V = 1$ this here just corresponds to $k = 1$. For other wavenumbers non-stationary patterns must result. This somewhat peculiar behaviour does, however, not seem to become mechanically important in the following and further discussion is therefore not given. The surface evolution mode, magnified in Fig. 2c, shows a typical resonance like behaviour: the largest growth rates appear close to those wavenumbers corresponding to the oscillator's resonance frequency.

3.1. Instability of the surface evolution modes

In this subsection all results presented refer to surface evolution modes. A brief discussion of the role of the vibration modes is postponed to the next subsection.

Example results of the analysis for spatially varying stiffness are shown in Figs. 3 and 4. Without loss of generality the wavenumber of the stiffness variation has been set to $\alpha = 0.05$. For presenting the key findings, a configuration of the system has been chosen, for which a spatially local analysis, assuming no spatial variation

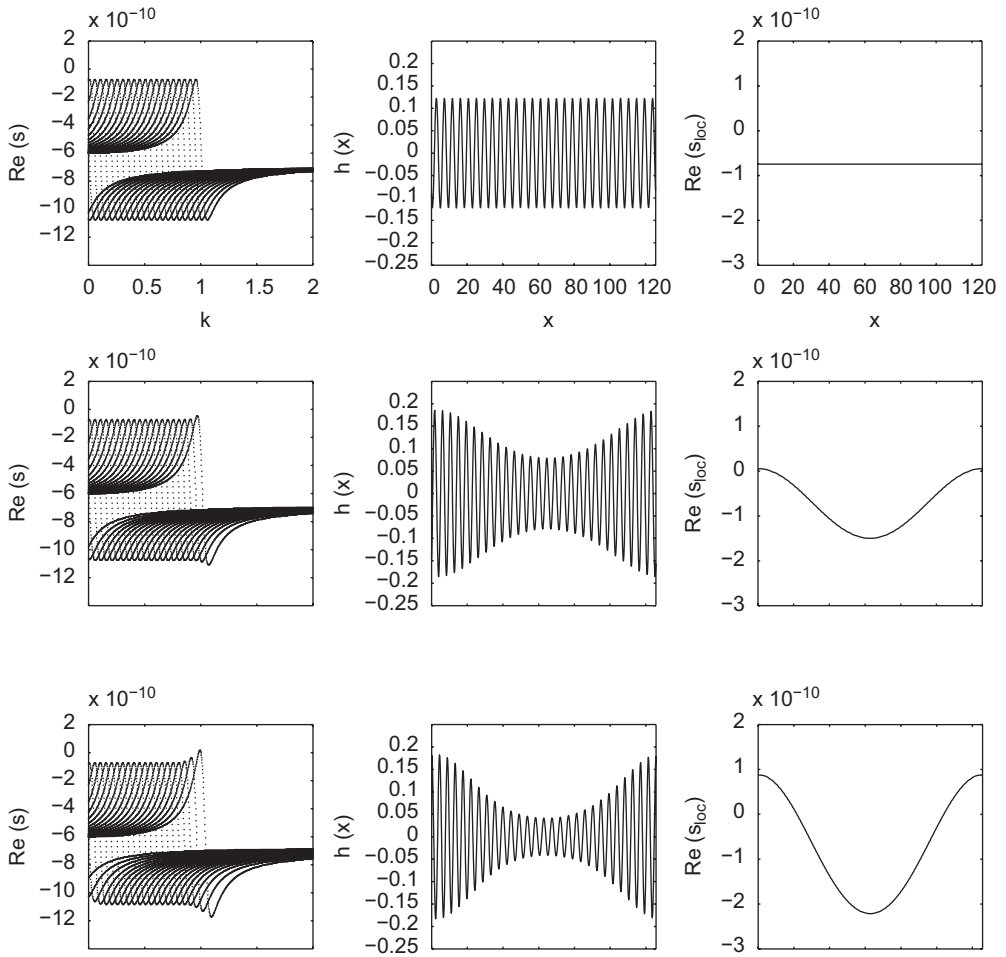

Fig. 3. Example results of Floquet analysis for $m = 1\,\mathrm{kg}$, $d/m = 1\,\mathrm{kg\,m\,s^{-1}}$, $\hat{\omega}_0 = 1\,\mathrm{s^{-2}}$, $V = 1\,\mathrm{m\,s^{-1}}$, $\beta = 6 \times 10^{-10}$, $a(H_0) = 1 \times 10^{-10}\,\mathrm{s\,kg^{-1}}$, $\alpha = 0.05\,\mathrm{m^{-1}}$. Left: the real part of the spectrum, i.e. the growth rates. In the middle: the surface-related part of the eigenvector for the strongest growing mode. Right: local growth rate corresponding to the local stiffness at a given position. From top to bottom the amplitude of parameter variation is increased: $\hat{\omega}_1 = 0.0, 0.05, 0.10\,\mathrm{s^{-2}}$.

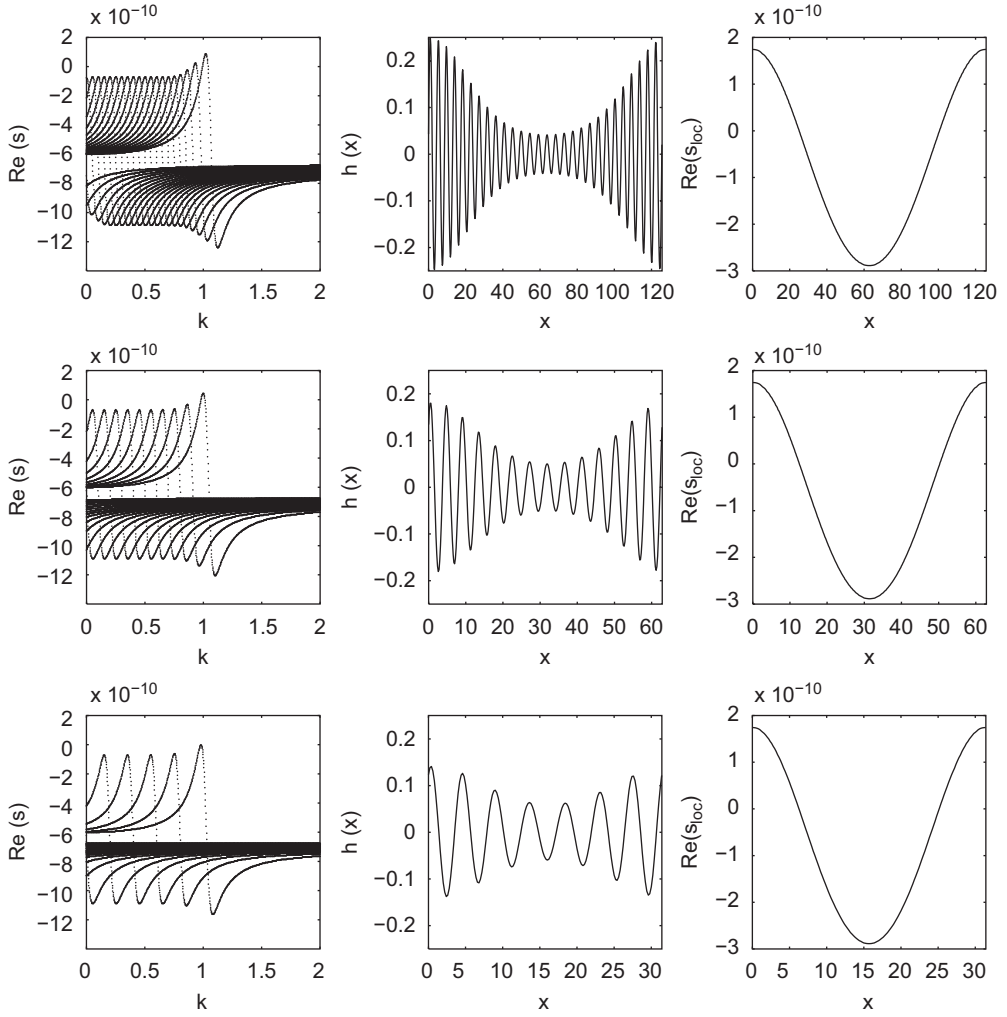

Fig. 4. Example results of Floquet analysis for $m = 1\,\mathrm{kg}$, $d/m = 1\,\mathrm{kg\,m\,s^{-1}}$, $\hat{\omega}_0 = 1\,\mathrm{s^{-2}}$, $\hat{\omega}_1 = 0.15\,\mathrm{s^{-2}}$ $V = 1\,\mathrm{m\,s^{-1}}$, $\beta = 6 \times 10^{-10}$, $a(H_0) = 1 \times 10^{-10}\,\mathrm{s\ kg^{-1}}$. Left: the real part of the spectrum, i.e. the growth rates. In the middle: the surface-related part of the eigenvector for the strongest growing mode. Right: local growth rate corresponding to the local stiffness at a given position. From top to bottom the wavenumber of parameter variation is increased: $\alpha = 0.05, 0.1, 0.2\,\mathrm{m^{-1}}$. Note the different scaling from top to bottom.

of stiffness, may give instability in a certain area, while stability in another area. In Fig. 3 the amplitude $\hat{\omega}_1 = \hat{\omega}_{-1}$ of the stiffness variation is increased from zero to non-zero values.

First of all one notes that there are many curves in the representation of the growth rates $\mathrm{Re}(s)$ (left column of Fig. 3). Each of these curves somewhat resembles the result shown in Fig. 2. The origin of this behaviour lies in a mathematical ambiguity the Floquet expansion brings along for vanishing periodicity: when there is no spatial variability of the underlying equations, and nevertheless a Floquet expansion with an arbitrary periodicity length is assumed, the assumption of a periodic Floquet expansion function and an exponential Floquet term does not uniquely specify the resulting eigensolutions: altogether a series expansion with terms like $\exp[\mathrm{i}(n\alpha + k)x]$ results; since the single expansion coefficients do decouple in the case of spatial homogeneity, the solution corresponding to a given expansion coefficient $\hat{n}$ and wavenumber $\hat{k}$ will then obviously be identical to the solution from the expansion coefficient $\tilde{n} = \hat{n} + m$ with the Floquet wavenumber $\tilde{k} = \hat{k} - m\alpha$, where m is a natural number. From this one may follow that the eigenvalue pattern for $n = 0$ (corresponding to the fundamental result) repeats itself towards smaller k-values with a periodicity length of α.

This degeneracy of the spectrum is, however, broken when a non-zero stiffness variation is admitted. Then instability results for certain Floquet wavenumbers around $k = 1$, i.e. the wavenumber to be expected also from the local analysis. The corresponding surface height components of the most unstable eigenvector are also presented in Figs. 3 and 4. Obviously corrugation with large amplitude results where also local analysis would have shown instability. However, also in those ranges where the local analysis shows stable behaviour, corrugation exists.

Fig. 4 shows the resulting behaviour when the wavenumber of the stiffness variation is increased. Note especially the change of the eigenvalue structure.

At first sight, the results obtained seem plausible and not really surprising: in areas where instability is predicted by assuming locally constant parameters, also the unstable Floquet modes show maximum wear pattern generation. In addition, a more detailed evaluation shows—although hardly visible from the graphs by the eye—that in regions of high stiffness the wear pattern wavelength is slightly shorter than in areas with lower stiffness.

An important question, however, remains: Is the effort related to a solution of the complete Floquet type problem justified, or would a local analysis based on local parameter values also be sufficient to adequately predict wear pattern growth? At least a partial solution to this question can be obtained by performing parameter studies. A comparison of results from a local analysis and from a Floquet analysis is presented in Fig. 5.

The parameters are varied in a systematic way by increasing the amplitude of the spatial stiffness variation. For vanishing variation the system is locally stable at every position and also the Floquet stability analysis predicts stable behaviour. When the amplitude of stiffness variation is increased, the system turns locally unstable. This goes back to the fact that larger stiffness leads to larger growth rates. To compare the results of Floquet analysis with local growth rates, Fig. 5 gives the maximum local growth rate obtained over one spatial period of the stiffness variation, the corresponding minimum local growth rate, as well as the horizontal average of the local growth rates. According to this analysis the system at hand turns locally unstable for the first time when the amplitude $\hat{\omega}_1$ of the stiffness variation reaches a value of about 0.09.

Now the question arises, whether local instability at a relatively small spatial interval is already sufficient to result in the growth of wear patterns. To answer this question maximum growth rates for the wavenumbers

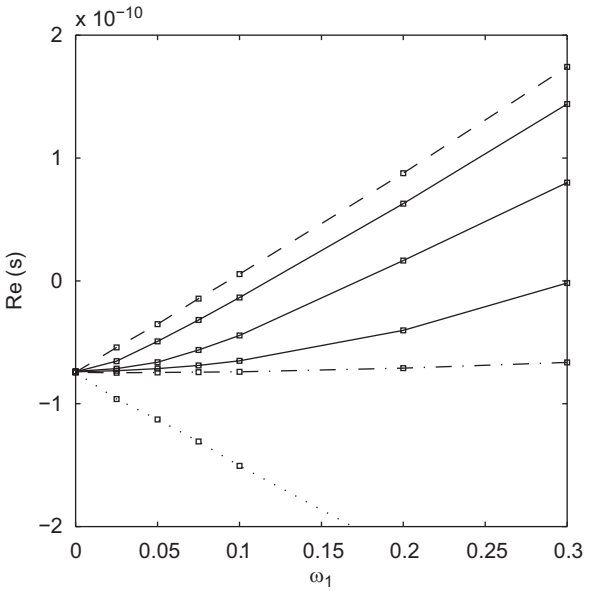

Fig. 5. Maximum growth vs. amplitude of stiffness variation. The dashed line gives the maximum local growth rate, the dotted line the minimum local growth rate, both evaluated by ignoring spatial inhomogeneity. The dash-dotted line shows the horizontally averaged local growth rate. Then, solid lines from top to bottom, the maximum growth rates vs. amplitude of parameter variation $\hat{\omega}_1$ are shown for different wavelengths of the parameter variation, namely $\alpha = 0.02, 0.05, 0.2\,\mathrm{m}^{-1}$.

$\alpha = 0.02, 0.05$ and $0.2\,\mathrm{m}^{-1}$ of the stiffness variation are shown in Fig. 5. One should note that these wavenumbers roughly correspond to 50, 20 and 10 wavelengths of the local wear pattern fitting into one period of the underlying stiffness variation. It turns out that for very large wavelengths of the parameter variation the resulting maximum growth rates approach the results of the local linear analysis. This seems plausible, since it could be expected that for very slow underlying parameter variations primarily the local properties of the system determine the emergence of patterns. However, even in the case of a ratio of 0.02 between the wavelength of wear pattern and parameter variation, the deviation in predicting the onset of pattern emergence is of the order of 20%. The closer the wavelength of parameter variation gets to the wavelength of the local wear pattern, the larger the predicted onset values become. E.g. for a ratio of 0.2 between the wavelength of wear pattern and parameter variation, the local prediction for wear pattern emergence would be about $\hat{\omega}_1 = 0.09\,\mathrm{s}^{-2}$, while Floquet analysis predicts a value of about $\hat{\omega}_1 = 0.30\,\mathrm{s}^{-2}$.

Qualitatively this behaviour could have been expected: when the underlying system changes its parameters "quickly", a local instability could just not have enough "time" or "space" to emerge as much as not to be overcome by the dissipative effects active in the locally stable areas. The phenomenon is very marked and thus could be interpreted as a stabilizing effect of parameter variations when keeping the maximum local growth rate constant. Asymptotically, when the wavelength of the parameter variation decreases strongly, the growth rates resulting from Floquet analysis decrease towards the growth rates corresponding to a spatial average of local growth rates.

It thus turns out that the true growth resulting from Floquet analysis is always bounded from above by the maximum local growth rate, and from below by the spatial average of the local growth rates. The bounding values are approached for asymptotically large and asymptotically small wavelengths of stiffness variation, respectively. The effect of introducing a variability in stiffness is potentially ambiguous; when starting with knowledge about the maximum local growth rate, it turns out that the true growth rate is always smaller than this maximum local growth rate; the variability thus could be interpreted to be stabilizing. When starting with knowledge about the average over local growth rates, however, it turns out that the true growth rate is always larger than that average value; from this point of view the variability could be interpreted to be destabilizing.

3.2. Parametric instability of the vibration modes

Within the context of the above analysis one may wonder how the results could be linked with the parametric instability also to be expected in the system. To clarify this point, a parameter study was performed in which wavenumber and amplitude of the stiffness variation were varied. Example results for $\alpha \approx 1\,\mathrm{m}^{-1}$, i.e. fundamental resonant forcing, are shown in Fig. 6.

As shown already at the beginning of this section, the eigenvalue analysis of the system yields modes that can be attributed to structural vibration, and modes that can be attributed to surface evolution. When a parametric resonance condition is met, e.g. for $\alpha \approx 1\,\mathrm{m}^{-1}$, parametric instability does indeed result for large enough amplitudes of the parameter variation. However, it is not the surface evolution modes that are destabilized, but modes belonging to the group of vibration modes. In Fig. 6 this parametric instability manifests itself by the positive growth rates which do not depend on the Floquet wavenumber k; what basically shows that the parametric instability is a purely temporal instability, not related to any truly spatial dynamics. The growth rates due to parametric instability are by several orders of magnitude larger than the growth rates of the surface evolution modes. Moreover it is quite surprising that the growth of the surface evolution modes themselves, which are also shown in Fig. 6, remains unaffected through parametric resonance.

It may therefore be concluded that the wear pattern instability presented in the preceding subsection and parametric instability due to parametric forcing are two independent instability mechanisms. Each mechanism is related to distinct branches in the spectrum of the system. While wear pattern instability is independent from parametric resonance conditions, parametric instability—as usual—depends strongly on the corresponding parameter combinations. E.g. Fig. 7 shows a typical stability diagram for parametric instability of the system, clearly demonstrating the typical tongue-like stability boundaries corresponding to fundamental, sub- and super-harmonic resonances: there is a number of resonances for $\alpha < 1\,\mathrm{m}^{-1}$, for which the parameter variation extends over a number of corrugation wavelengths; the smaller the corresponding α, the larger the necessary

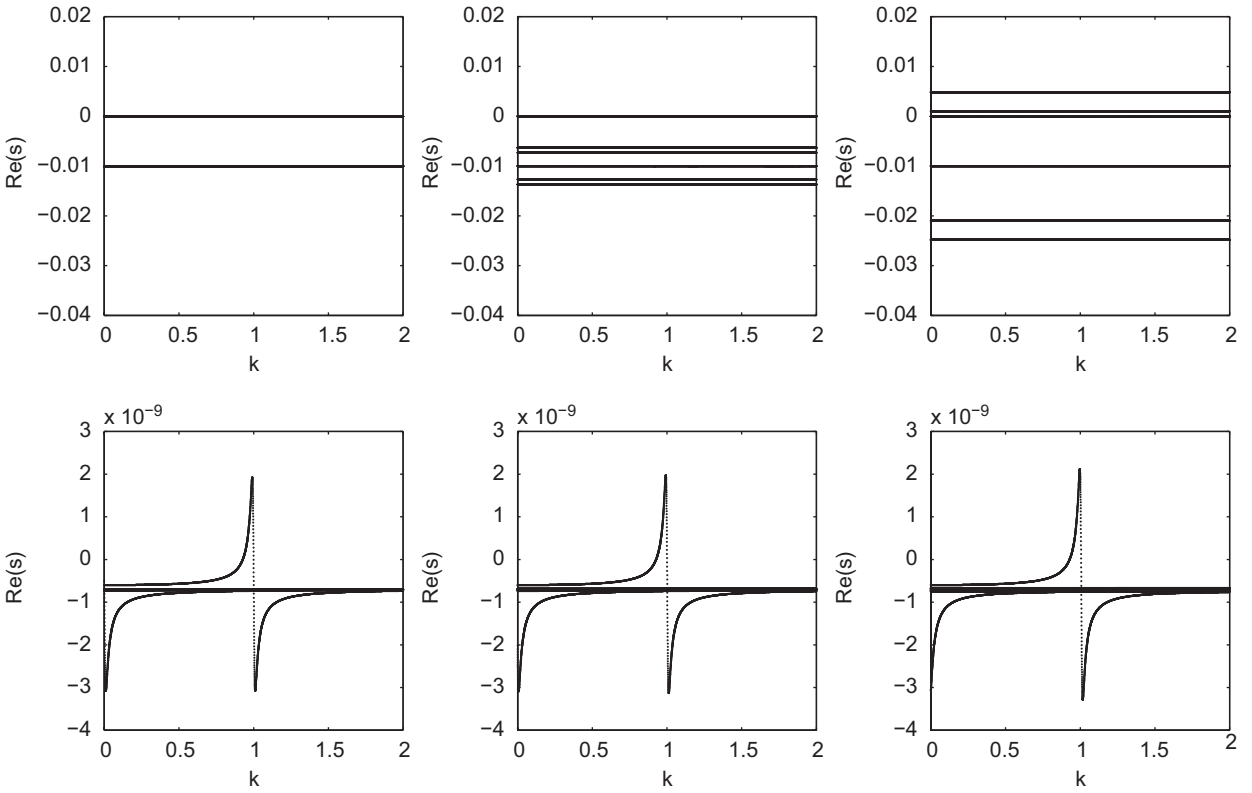

Fig. 6. Growth rates at fundamental parametric forcing. $m = 1\,\mathrm{kg}$, $d/m = 0.02\,\mathrm{kg\,m\,s^{-1}}$, $\hat{\omega}_0 = 1\,\mathrm{s^{-2}}$, $V = 1\,\mathrm{m\,s^{-1}}$, $\beta = 6 \times 10^{-10}$, $a(H_0) = 1 \times 10^{-10}\,\mathrm{s\,kg^{-1}}$, $\alpha = 1.0\,\mathrm{m^{-1}}$, $\hat{\omega}_1 = 0.0$ (left), 0.1 (middle), $0.2\,\mathrm{s^{-2}}$ (right). Both the full spectrum of growth rates (top), as well as the surface evolution modes in extended scaling (bottom) are shown.

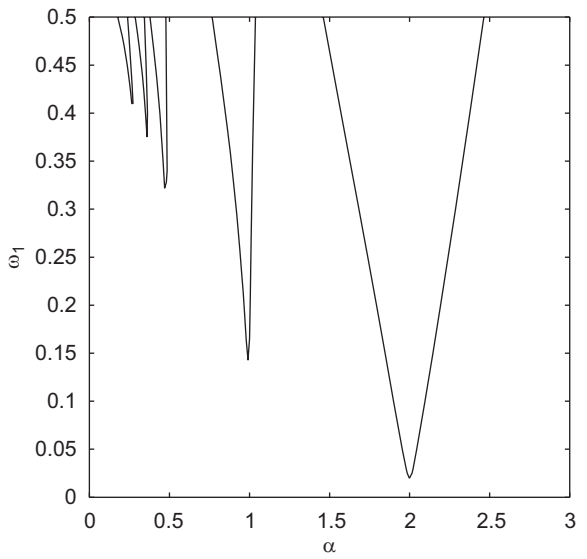

Fig. 7. Stability map for parametric instability. $m = 1\,\mathrm{kg}$, $d/m = 0.02\,\mathrm{kg\,m\,s^{-1}}$, $\hat{\omega}_0 = 1\,\mathrm{s^{-2}}$, $V = 1\,\mathrm{m\,s^{-1}}$, $\beta = 6 \times 10^{-10}\,\mathrm{s^{-1}}$, $a(H_0) = 1 \times 10^{-10}\,\mathrm{s\,kg^{-1}}$.

amplitude $\hat{\omega}_1$ to destabilize the system. Then there is the fundamental resonance with $\alpha \approx 1\,\mathrm{m}^{-1}$, and there is a marked instability for $\alpha \approx 2\,\mathrm{m}^{-1}$, where about two periods of the parameter variation extend over a single wavelength of the "natural" corrugation wavelength. One should note, as is often the case in parametric resonance, that the fundamental resonance (i.e. $\alpha \approx 1\,\mathrm{m}^{-1}$) is not the most critical case; the instability with $\alpha \approx 2\,\mathrm{m}^{-1}$ appears for smaller amplitudes $\hat{\omega}_1$.

Of course, parametric instability will also be accompanied by wear pattern formation—the parametrically forced vibration will leave its footprints on the surface. Nevertheless wear pattern formation during parametric instability has to be regarded as a mechanism different from the wear pattern instability in the absence of parametric forcing. The above results of the Floquet type analysis on the effect of long-wavelength parameter variations on wear pattern formation may therefore be considered as unrelated to parametric instability. A more detailed analysis of wear pattern generation due to parametric forcing itself is left for future studies. As a consequence of the present work it seems, however, sufficient to analyse parametrically driven wear pattern formation with the classical analysis tools for parametrically driven oscillations (as e.g. in Ref. [14] for a related system). In addition, certainly nonlinear aspects of limit-cycle formation, contact loss, etc. will then have to be taken into account, which by far exceeds the scope of the present study.

4. Summary, conclusions and outlook

The present work addresses the influence of spatial parameter dependencies on wear pattern generation. Using a simple generic minimal model a harmonic stiffness variation of the structural system is assumed. Applying Floquet stability theory it is shown that a spatial variation of stiffness has a stabilizing effect, when local maximum growth rates are taken as a comparative basis. When the wavelength of the underlying parameter variation is asymptotically long compared to the wavelength of the wear pattern expected from the homogeneous system, the stability boundaries obtained from regarding the local, non-varying parameters only, seem sufficient. When the wavelength of the parameter dependency does, however, reach the order of magnitude of the wear pattern wavelength, the parameter variations will tend to substantially stabilize the system and spatially averaged local growth rates will asymptotically determine the stability boundary. For general parameter conditions, however, a spatially local analysis of the stability properties alone will usually not capture stability boundaries for wear pattern generation properly. Only a full analysis based on Floquet theory will give correct predictions.

In addition, it has been shown that parametric resonance, possibly with accompanying wear pattern generation, is an effect independent from wear pattern generation in the absence of parametric resonance.

The present work is of course based on a highly simplified model for both the structural as well as the tribological system. A more problem-specific extension of the rather schematic approach presented therefore seems highly necessary to better evaluate the true differences in predicting wear pattern emergence from using a local or a full analysis. In addition, a more detailed investigation of wear pattern generation during parametric excitation should be conducted.

Among the needs on better and extended modelling, just a few should be mentioned: (1) Other parameter dependencies: In the present work merely a harmonic stiffness variation has been taken into account. Non-harmonic variations, as well as variations of other parameters, like e.g. damping, could, however, yield further effects, calling for an extension of the approach. (2) Structural modelling: The role of nonlinearities in the structural system has not been investigated in the present context. This might, however, often be relevant; especially in the case of parametric instability, or due to nonlinear stiffness characteristics possibly arising from contact mechanics. Also, should the approach be applied to rolling contact, more adequate contact mechanics models should be used. (3) Wear modelling: The Archard type wear is a highly simplified model for wear. Depending on the specific application, more appropriate models have to be applied. (4) Finite size wear regions: In many technically relevant systems the surface subjected to wear is finite, e.g. in friction brakes the brake disk is characterized by a finite circumferential length. The present analysis for infinitely extended systems can easily be extended to such finite systems by constraining the allowable wavenumbers for both the underlying parameter dependency, as well as the wear pattern to the discrete set of values corresponding to the underlying periodic boundary conditions. (5) Nonlinear surface topography evolution: The approach presented is a linear stability analysis. Questions with respect to amplitude saturation, i.e. finite-amplitude

issues, are not addressed. For growing surface corrugation such finite-amplitude effects might become important.

In addition to the modelling related open points, there are also a number of additional conceptual questions still to be answered. The problem of wear pattern emergence is a spatio-temporal problem with advective characteristics due to the contact partners in relative motion. From e.g. plasma physics and fluid dynamics (e.g. Ref. [15]) it has been known for many years that next to the straightforward questions of the usual—the so-called temporal—stability analysis used, also spatial aspects concerning the propagation of perturbations may play a role. Especially when the systems are open, as e.g. in the case of roads or rails, disturbances might grow, according to temporal linear stability analysis; the growing perturbations within a given spatial interval might, however, be convectively carried away downstream to areas where they could be damped away again. These so-called "convective instabilities" are markedly different from the so-called "absolute instabilities" which after the initiation of growth affect the whole spatial domain. In some research fields with open systems and strongly advective effects it has turned out that it is actually not the onset of temporal linear instability, but the transition between convective and absolute instability that determines the appearance of patterns. In addition, one could mention that next to the traditional linear stability considerations in recent years non-modal stability aspects have gained importance for open advection affected systems (e.g. Ref. [16]). Studies on these related alternative mechanisms seem necessary, especially with a view to the still prevailing deficiencies in correctly delimiting parameter regimes of wear pattern emergence.

References

[1] J.A. Both, D.C. Hong, D.A. Kurtze, Corrugation of roads, *Physica A* 301 (2001) 545.
[2] N.P. Hoffmann, M. Misol, On the role of varying normal load and of randomly distributed relative velocities in the wavelength selection process of wear-pattern generation, *International Journal of Solids and Structures* 44 (2007) 8718.
[3] Y. Sato, A. Matsumoto, K. Knothe, Review on rail corrugation studies, *Wear* 253 (2002) 130.
[4] S.L. Grassie, J. Kalousek, Rail corrugations. Characteristics, causes and treatments, *Journal of Rail Rapid Transit* 207 (1993) 57.
[5] A. Bhaskar, K.L. Johnson, G.D. Wood, J. Woodhouse, Wheel-rail dynamics with closely conformal contact. Part 1: dynamic modelling and stability analysis, *Journal of Rail Rapid Transit* 211 (1997) 11.
[6] C.O. Frederick, W.G. Bugden, Corrugation research on British Rail, in: K. Knothe (Ed.), *Symposium on Rail Corrugation Problems*, *ILR-Bericht*, Vol. 56, Technische Universität, Institut für Luft- und Raumfahrt, Berlin, 1983.
[7] S. Grassie, J. Edwards, J. Shepherd, Roaring rails. An enigma largely explained, *International Railway Journal* 47 (2007) 31.
[8] G. Diana, F. Cheli, S. Bruni, A. Collina, Experimental and numerical investigation on subway short-pitch corrugation, *Vehicle System Dynamics* 29 (1998) 234.
[9] N. Taberlet, S.W. Morris, J.N. McElwaine, Washboard road: the dynamics of granular ripples formed by rolling wheels, *Physical Review Letters* 99 (2007) 068003.
[10] G. Floquet, Sur les équations différentielles linéairesà coefficients périodiques, *Annales de'lÉcole Normale Superieure* 12 (1883) 47.
[11] D.A. Kurtze, D.C. Hong, J.A. Both, The genesis of washboard roads, *International Journal of Modern Physics B* 15 (2001) 3344.
[12] P.J. Bolton, P. Clayton, I.J. McEwen, Wear of rail and tyre steels under rolling/sliding conditions, *ASLE Transactions* 25 (1982) 1724.
[13] P.J. Bolton, P. Clayton, Rolling-sliding wear damage in rail and tyre steels, *Wear* 93 (1984) 145.
[14] T.X. Wu, M.J. Brennan, Basic analytical study of pantograph-catenary system dynamics, *Vehicle System Dynamics* 30 (1998) 443.
[15] P. Huerre, Local and global instabilities in spatially developing flows, *Annual Review of Fluid Mechanics* 22 (1990) 473.
[16] F. Waleffe, Transition in shear flows—nonlinear normality versus nonnormal linearity, *Physics of Fluids* 7 (1995) 3060.